Optics Letters

Narrow-linewidth self-injection locked diode laser with a high-Q fiber Fabry–Perot resonator

LIYUN HAO,[1] XIAOHAN WANG,[1] DONGJIE GUO,[1] KUNPENG JIA,[1] PENGFEI FAN,[1] JIAN GUO,[1] XIN NI,[1] GANG ZHAO,[1,2] ZHENDA XIE,[1,*] AND SHI-NING ZHU[1]

[1]*National Laboratory of Solid State Microstructures, School of Electronic Science and Engineering, College of Engineering and Applied Sciences, and School of Physics, Nanjing University, Nanjing 210093, China*
[2]*e-mail: zhaogang@nju.edu.cn*
**Corresponding author: xiezhenda@nju.edu.cn*

Received 8 January 2021; revised 4 February 2021; accepted 8 February 2021; posted 16 February 2021 (Doc. ID 415859); published 11 March 2021

Narrow-linewidth lasers are essential for various applications, but are limited by their size, weight, power, and cost requirements. Here we demonstrate a self-injection locked diode laser fabricated with a high quality factor fiber Fabry–Perot resonator, with a 145 Hz free-running linewidth. The locking scheme is all-fiber for plug-and-play operation. White frequency noise of 50 Hz^2/Hz is measured with over 42 dB reduction from the low-cost TO-can distributed feedback laser diode, and shows its wide applications in a compact and cost-effective way.

https://doi.org/10.1364/OL.415859

The narrow-linewidth lasers not only push the frontiers in optics such as optical clocks and gravitational wave detection [1–3], but also enable extensive applications, including high-precision-laser lidars, coherent optical communications, and distributed fiber optical sensing [4–6]. These practical applications call for laser systems with low size, weight, power, and cost (SWaP-C), which may be achieved by the diode lasers. However, the normal diode lasers suffer from their relatively broad linewidth. Most monolithic laser diodes have a limited linewidth at megahertz level, even with the extra efforts on the chip–scale fabrication such as distributed feedback (DFB) or Bragg reflector structures [7–11]. Extend cavity lasers with external feedback can greatly reduce the linewidth to kilohertz level, and active locking mechanism can further reduce the linewidth. However, these techniques involve either bulk-element optical loops or complex electronics, which add to the SWaP-C and reduce the robustness of the whole system [12–14].

On the other hand, self-injection locking from an external narrow-band optical filter can greatly reduce the linewidth of an existing laser diode [15–19]. No electronic feedback control is required in this scheme, and significant linewidth reduction is possible in a compact setup, taking advantage of the fast-developing microresonator technology. For example, a high quality factor (Q) up to 10^{11} can be achieved from a whispering gallery mode (WGM) resonator for self-injection locking using back scattering inside the resonator, and a narrow spectral linewidth can be achieved as low as 30 Hz [18]. However, the WGM resonators require sophisticated coupling techniques such as prism coupling or a tapered fiber. Fine alignment of free-space optics is also required.

In this Letter, we demonstrate a self-injection locked diode laser using a high-Q fiber Fabry–Perot (FFP) resonator with Q of 3.95×10^7. Such an FFP resonator is fabricated with commercially available fiber and mounted with ceramic ferrules on both fiber ends, which can be compatible with standard PC type fiber connectors for plug-and-play operation in an all-fiber feedback loop. The source laser we use is a low-cost DFB diode in a standard TO-can package for telecom application, powered by an ordinary constant-current laser driver. A free-running, laser spectral linewidth of 145 Hz is measured, with white frequency noise of 50 Hz^2/Hz, which is reduced by over 42 dB from the unlocked DFB laser diode. This result presents a straightforward and cost-effective way to access an ultra-narrow linewidth for broad applications requiring high coherence in a compact package and high robustness.

In the experiment, the FFP resonator is made from highly nonlinear fiber (HNLF) with a fiber length of 6.8 cm and a mode field diameter of 4 μm. Both fiber ends are mounted in ceramic ferrules and finely polished with sub-nanometer surface roughness. Ten-layer pairs of TiO_2 and SiO_2 are then coated using an ion-assisted deposition method to achieve a reflectivity of over 99.6% from 1530 to 1570 nm [20]. Plug-and-play operation can be achieved with commercial ceramic sleeves for fiber pigtailed connector on both ends, as shown in Fig. 1(a). A tunable external-cavity diode laser possessing linewidth of 1 kHz is used to characterize the FFP resonator by scanning the laser frequency across the resonances. A fiber polarization controller is used at the input port to match the laser polarization to one set of polarization modes of the FFP resonator. At a relatively large free spectral range of 1.5 GHz, a narrow resonance linewidth of 4.9 MHz is measured, showing a high finesse of 306 and a Q factor of 3.95×10^7. Such high finesse is beneficial to achieve a high linewidth narrowing factor for the self-injection while keeping the single-mode (SM) lasing.

The experimental setup of the self-injection locked laser with the FFP resonator is schematically shown in Fig. 2. The source laser (LD) is a standard telecom DFB laser diode at 1549.1 nm

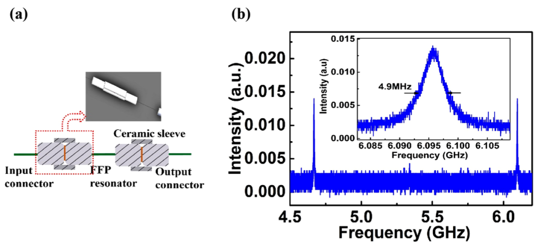

Fig. 1. (a) Cross-sectional drawing of the plug-and-play operation of the FFP resonator. The inset shows how the ceramic sleeve holds the ferrules together for both the FFP resonator and the input/output connector. (b) Characterization of the FFP resonator, transmission signals when scanning a lower-power narrow-linewidth laser across the resonances. Inset, zoom-in of one resonance peak.

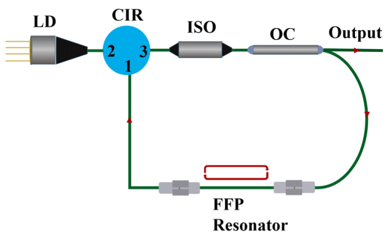

Fig. 2. Setup of the all fiber self-injection locked laser. LD, source laser; CIR, optical circulator; ISO, optical isolator; OC, optical coupler.

with a low-cost TO-can package. It has no built-in isolator (ISO) and is SM fiber pigtailed with an in-fiber output power of 4 mW when driven by an ordinary constant-current power supply at 36 mA current. The laser emission is injected to port 2 of a three-port circulator (CIR), with port 3 connecting to an ISO for better isolating back scattering light from films of the FFP resonator. It is then launched to a 50/50 optical coupler (OC) to divide into two parts, where 50% is served as output power of the laser, and the rest is direct to the input of the FFP resonator. Here the FFP resonator acts as a narrowband filter, and its resonant transmission feeds back to the laser cavity through port 1 of the CIR, leading to self-injection locking of the source laser. The overall fiber feedback loop is about 1.25 m long. No active temperature control or vibration shielding is used for either the laser diode or the FFP resonator. The output power of the locked laser is measured to be 1.8 mW with a power meter.

We use delayed self-heterodyne interferometry (DSHI) to measure the linewidth performance of the self-injection locked laser. Figure 3(a) shows the measurement setup utilizing a fiber Mach–Zehnder interferometer (MZI) structure. The measured beam is equally split into two parts by fiber coupler C1 (50/50). One part is delayed by 13244 m SM fiber, and the other goes through an acoustic optical modulator (AOM) to generate a 40 MHz frequency shift for avoiding strong zero frequency noise. The two parts are recombined by fiber coupler C2 (50/50) and fed into a photodetector (PD). An electrical spectrum analyzer (ESA) is used to analyze the beating signal acquired.

First we measure the spectral linewidth of the source laser under non-locked case. With a scanning span of 5–75 MHz and resolution of 100 Hz of the ESA, the radio frequency (RF) spectrum of the source laser is shown in the black curve of Fig. 3(b). Its Lorentz fitting characterizes a 3 dB width of 3.03 MHz,

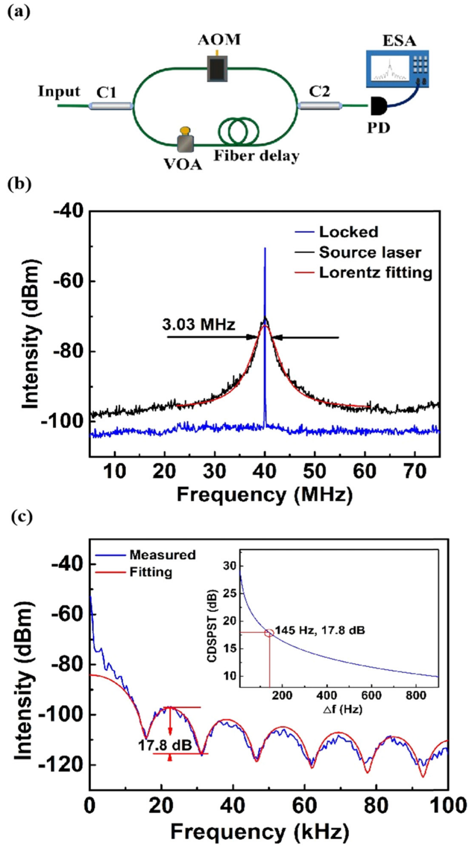

Fig. 3. Linewidth characterization. (a) Measurement setup. C1 & C2, 50/50 fiber coupler. VOA, variable optical attenuator to adjust the same power in two arms of the DSHI. AOM, acoustic optical modulator; ESA, electrical spectrum analyzer; PD, photodetector. (b) Dramatic linewidth reduction of the self-injection locking. Black curve, RF spectrum of the source diode. Red curve, Lorentz fitting. Blue curve, RF spectrum of the locked state. (c) Linewidth calculated from the envelope of sub-coherence self-heterodyne. Blue curve, measured coherent envelope. Red curve, numerical fitting. Inset, calculated relationship between the measured linewidth and value of CDSPST at a 13244 m fiber delay.

which indicates that the spectral linewidth of the source laser is ∼1.52 MHz. Using the same measurement setup, drastic narrowing of the RF spectrum is observed after self-injection locking to the FFP resonator [blue curve of Fig. 3(b)]. Indeed, the locked linewidth is so narrow that it is beyond the non-coherence limit of a relatively short delaying fiber length of 13244 m. Strong oscillations and a sharp peak are observed after zooming in on the RF spectrum of the locked state, where the conventional Lorentz fitting is impossible.

To get a laser linewidth of the locked state, a sub-coherence envelope comparison based on short delayed self-heterodyne interferometry (SDSHI) is adopted. This technique was proposed in recent years for ultra-narrow-linewidth measurement using a fiber delay shorter than its coherent length. The laser linewidth can be obtained by fitting the strong coherent envelope or comparing the contrast difference between the second peak and the second through (CDSPST) [21,22]. The coherent envelope measured (blue curve) and numerical calculated (red curve) based on the theoretical power spectrum density using SDSHI are shown in Fig. 3(c). The full envelope is symmetrical;

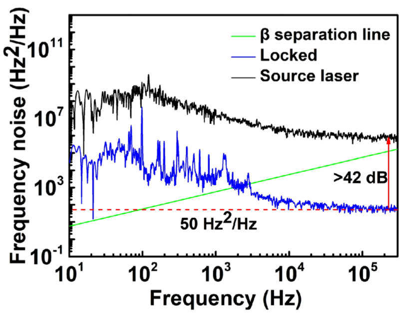

Fig. 4. PSD of the frequency noise spectrum of the source laser (black curve) and under a locked state (blue curve). β separation line is given by $S_\upsilon(f) = 8 \times \ln 2 \times f/\pi^2$ [24], where f is the Fourier frequency.

in the picture, it has been frequency offset by 40 MHz to center the peak at 0 MHz. Auto optimization is done, and the best fitting is achieved with a laser linewidth set of 145 Hz. This fitting result is consistent with that calculated from the measured 17.8 dB CDSPST, as shown in the curve of calculated CDSPST versus the laser linewidth in the inset of Fig. 3(c).

The differential phase noise of the laser is also investigated based on the above DSHI setup with 35 m delayed fiber [23]. Figure 4 shows transformed single-sided power spectral density (PSD) of the frequency noise of the source laser (black curve) and under a locked state (blue curve). Under self-injection locking, both low-frequency $1/f$ noise and high-frequency white noise are well suppressed in the measured frequency range of 10 Hz–300 kHz, even with some noise spikes occurring below ∼1 kHz. These low-frequency spikes may arise from environmental disturbance, since no temperature controller or vibration isolation is used in this laser setup. The frequency noise measures at a constant value of 50 Hz^2/Hz above 30 kHz of the frequency range, showing a noise suppression efficiency over 42 dB from the source laser. This corresponds to an instantaneous laser linewidth of 157 Hz, which is in constant with the measured 145 Hz laser linewidth. We compare our experimental results with its theoretical expectation, using the following equation [25]:

$$\Delta\nu = \frac{\Delta\nu_0}{\left[1 + (1+\alpha^2)^{1/2}\sqrt{\beta}\frac{Q_p}{Q_d}\right]^2}, \tag{1}$$

where $\Delta\nu_0$ and $\Delta\nu$ are the spectral linewidths of the laser with and without self-injection locking, respectively. Q_p and Q_d are the quality factors of the FFP resonator and the laser diode cavity, which are measured to be 3.95×10^7 and 4×10^3, respectively. $\alpha = 2.5$ is the phase-amplitude coupling factor of the source laser. $\beta = 1.2 \times 10^{-3}$ is the power mode coupling factor [25], evaluated from on-resonance transmission (2.3%) of the FFP resonator and the transmission efficiency of other elements in the feedback loop. A linewidth reduction factor of 4.9×10^5 can be calculated for a laser linewidth limit at 2 Hz. This linewidth limit reveals the potential further linewidth reduction using the same resonator, and the nonperfect linewidth may be because of the technical noise in the current setup such as the electronic noise from the laser driver and the temperature fluctuation. Our experimental setup is only operated on an optical table with no shielding, which is inevitably influenced by environmental noise such as acoustical vibration. Even better performance of the laser can be expected after packaging it and shorting the feedback loops with more integrated components. Here we choose a 50/50 output coupling, considering a tradeoff between output power and the linewidth narrowing. A larger output-coupling ratio can be used with smaller loss in the feedback loop by improving the coupling efficiency of the FFP resonator or better splicing loss in fibers. Additionally, a more powerful laser source can be adopted to get higher output power.

In conclusion, we have demonstrated a 100 Hz level linewidth self-injection locked laser with a plug-and-play FFP resonator and no temperature controller. A 145 Hz spectral linewidth is obtained from the 1.52 MHz non-locked linewidth of a low-cost TO-can DFB laser diode. The low-frequency noise level of 50 Hz^2/Hz is measured at frequencies above 30 kHz with over 42 dB suppression. In this experiment, we use a HNLF-based FFP resonator that is originally designed for nonlinear optical application. In the future, the SM fiber-based FFP resonator can be used for an even lower noise limit and higher coupling efficiency. This method can also be easily adapted to any other wavelength and fulfills the requirements of narrow-linewidth lasers in a compact and cost-effective way.

Funding. National Key Research and Development Program of China (2017YFA0303700, 2019YFA0705000); National Natural Science Foundation of China (11621091, 11627810, 11674169, 11690031, 51890861, 91950206); Natural Science Foundation of Jiangsu Province (BK20192001); Key R&D Program of Guangdong Province (2018B030329001); Excellent Research Program of Nanjing University (ZYJH002).

Disclosures. The authors declare no conflicts of interest.

REFERENCES

1. C. W. Chou, D. B. Hume, T. Rosenband, and D. J. Wineland, Science **329**, 1630 (2010).
2. The LIGO Scientific Collaboration, Nat. Phys. **7**, 962 (2011).
3. A. L. Schawlow and C. H. Townes, Phys. Rev. **112**, 1940 (1958).
4. J. P. Cariou, B. Augere, and M. Valla, C. R. Phys. **7**, 213 (2006).
5. K. Kasai, Y. Wang, D. O. Otuya, M. Yoshida, and M. Nakazawa, Opt. Express **23**, 28423 (2015).
6. K. Numata, J. Camp, M. A. Krainak, and L. Stolpner, Opt. Express **18**, 22781 (2010).
7. C. H. Henry, IEEE J. Quantum Electron. **18**, 259 (1982).
8. C. Harder, K. Vahala, and A. Yariv, Appl. Phys. Lett. **42**, 328 (1983).
9. E. D. Hinkley and C. Freed, Phys. Rev. Lett. **23**, 277 (1969).
10. K. Vahala and A. Yariv, IEEE J. Quantum Electron. **19**, 1102 (1983).
11. K. Vahala and A. Yariv, IEEE J. Quantum Electron. **19**, 1096 (1983).
12. G. M. Smith, J. S. Hughes, R. M. Lammert, M. L. Osowski, G. C. Papen, J. T. Verdeyen, and J. J. Coleman, IEEE Photonics Technol. Lett. **8**, 476 (1996).
13. J. Alnis, A. Matveev, N. Kolachevsky, T. Udem, and T. W. Hänsch, Phys. Rev. A **77**, 053809 (2008).
14. K. Liu and M. G. Littman, Opt. Lett. **6**, 117 (1981).
15. Z. Xie, W. Liang, A. A. Savchenkov, J. Kim, J. Burkhart, M. McDonald, T. Zelevinsky, V. S. Ilchenko, A. B. Matsko, L. Maleki, and C. W. Wong, Opt. Lett. **40**, 2596 (2015).
16. F. Wei, F. Yang, X. Zhang, D. Xu, M. Ding, L. Zhang, D. Chen, H. Cai, Z. Fang, and G. Xijia, Opt. Express **24**, 17406 (2016).
17. W. Liang, V. S. Ilchenko, A. A. Savchenkov, A. B. Matsko, D. Seidel, and L. Maleki, Opt. Lett. **35**, 2822 (2010).
18. W. Liang, V. S. Ilchenko, D. Eliyahu, A. A. Savchenkov, A. B. Matsko, D. Seidel, and L. Maleki, Nat. Commun. **6**, 7371 (2015).
19. A. A. Savchenkov, S. Chiow, M. Chasemkhani, S. Williams, N. Yu, R. C. Stirbl, and A. B. Matsko, Opt. Lett. **44**, 4175 (2019).

20. K. Jia, X. Wang, D. Kwon, J. Wang, E. Tsao, H. Liu, X. Ni, J. Guo, M. Yang, X. Jiang, J. Kim, S. Zhu, Z. Xie, and S.-W. Huang, Phys. Rev. Lett. **125**, 143902 (2020).
21. S. Huang, T. Zhu, Z. Cao, M. Liu, M. Deng, J. Liu, and X. Li, IEEE Photonics Technol. Lett. **28**, 759 (2016).
22. S. Huang, T. Zhu, M. Liu, and W. Huang, Sci. Rep. **7**, 41988 (2017).
23. W. Ma, B. Xiong, C. Sun, X. Ke, Z. Hao, L. Wang, J. Wang, Y. Han, H. Li, and Y. Luo, Appl. Opt. **58**, 3555 (2019).
24. G. D. Domenico, S. Schilt, and P. Thomann, Appl. Opt. **49**, 4801 (2010).
25. P. Laurent, A. Clairon, and C. Bréant, IEEE J. Quantum Electron. **25**, 1131 (1989).